

Cyberkelp: an integrative approach to the modelling of flexible organisms

Mark W. Denny* and Ben B. Hale

Hopkins Marine Station of Stanford University, Pacific Grove, CA 93950, USA

Biomechanical models come in a variety of forms: conceptual models; physical models; and mathematical models (both of the sort written down on paper and the sort carried out on computers). There are model structures (such as insect flight muscle and the tendons of rats' tails), model organisms (such as the flying insect, *Manduca sexta*), even model systems of organisms (such as the communities that live on wave-swept rocky shores). These different types of models are typically employed separately, but their value often can be enhanced if their insights are integrated. In this brief report we explore a particular example of such integration among models, as applied to flexible marine algae. A conceptual model serves as a template for the construction of a mathematical model of a model species of giant kelp, and the validity of this numerical model is tested using physical models. The validated mathematical model is then used in conjunction with a computer-controlled tensile testing apparatus to simulate the loading regime placed on algal materials. The resulting information can be used to create a more precise mathematical model.

Keywords: kelp; *Nereocystis*; model; ocean waves; hydrodynamic forces

1. THE PROBLEM

As ocean waves approach a rocky coast, they subject the plants and animals of the shore to rapid water velocities. For example, a typical surface wave 2 m high travelling in water that is 10 m deep is accompanied by a water velocity of 1.1 m s^{-1} . Under storm conditions (during which waves at this depth may reach a breaking height of 7–8 m), the water velocity may be as high as 3.8 m s^{-1} . These velocities are capable of imposing large hydrodynamic forces on subtidal nearshore organisms (Witman 1987; Massel & Done 1992; Friedland & Denny 1995; Denny 1995; Gaylord & Denny 1997; Kawamata 1998, 2001). In apparent response to this loading, most wave-swept benthic organisms are small. For example, the largest animals commonly found on wave-swept shores are sea stars, which typically have a diameter of less than 20 cm, and most wave-swept plants have fronds less than 1 m long. The giant kelps, however, are a conspicuous exception. These brown algae are characteristic inhabitants of many of the most wave-battered shores on the planet, but they can grow to lengths of 40 m and have masses in excess of 50 kg (Foster & Schiel 1985). Furthermore, the giant kelps are constructed of relatively weak materials. Unlike the shells of molluscs, which have a breaking strength of 50–100 MPa (Currey 1978), or the byssal threads of mussels, which have a breaking strength of 50–75 MPa (Bell & Gosline 1996), the frond material of giant kelps has a breaking strength of only 3–5 MPa. The question then arises: how does an alga made from a weak material not only survive in one of the most physically stressful

environments on Earth, but also manage to grow to a size 10–100 times that of its neighbours?

The answer to this question is not of purely academic interest. Giant kelps are the source of a variety of economically important products, such as the alginates used in toothpastes, ice cream and shampoos, and 'forests' of these kelps are the nursery grounds for many commercial fish species (Foster & Schiel 1985). If we can understand how giant kelps survive in today's wave climate, we may gain an ability to predict how these plants will fare if (as predicted by some climate models, e.g. Goldenberg *et al.* 2001) the world's oceans become wavier in coming decades.

2. THE MODEL SPECIES

There are several species of subtidal giant kelps scattered widely throughout the oceans. *Macrocystis pyrifera* (giant kelp) is found on the west coasts of North and South America and in New Zealand, Australia and South Africa. *Eklonia maxima* is found on the west coast of South Africa, while *Pelagophycus porra* (elk kelp) is confined to the coasts of California and Mexico. It would be a daunting task to understand the complete mechanics of this morphologically diverse set of plants under the physically diverse conditions in which they are found. Instead, we approach the problem through the use of a single model species chosen for the simplicity of its structure.

Nereocystis leutkeana, the bull kelp (figure 1), lives on the west coast of North America from southern Alaska to Point Conception in California (Abbott & Hollenberg 1976). It consists of three major structural components:

- (i) a holdfast that serves to tether the plant to the substratum;
- (ii) a rope-like stipe that ends in a gas-filled, buoyant float, the pneumatocyst; and

* Author for correspondence (mwdenny@leland.stanford.edu).

One contribution of 20 to a Theme Issue 'Modelling in biomechanics'.

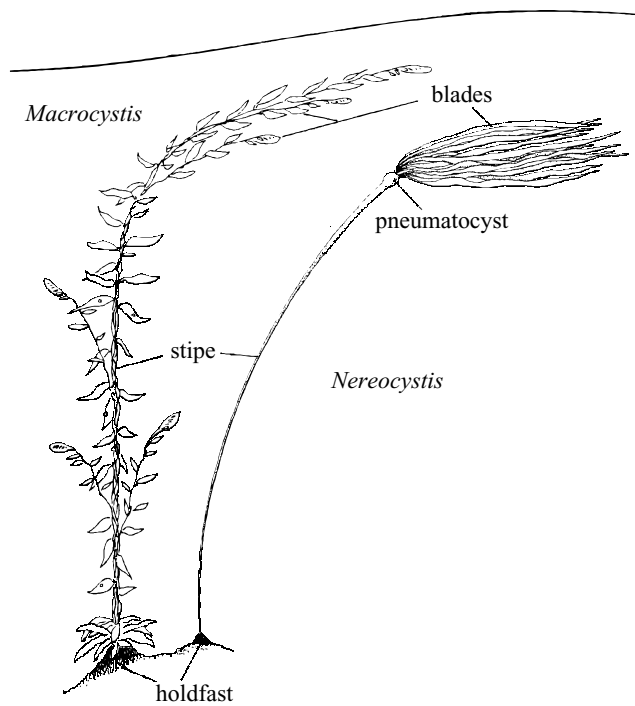


Figure 1. Giant kelps. The morphology of these two species spans the range of mechanical complexity seen in giant kelps. *Macrocyctis pyrifera* has blades distributed along the entire length of the stipe, and each blade has at its base a small pneumatocyst. Each holdfast can anchor multiple stipes. By contrast, the frond of *Nereocystis leutkeana* is much simpler: each holdfast has a single stipe which in turn bears a single, large pneumatocyst from which blades emerge.

- (iii) a set of 30–40 blades, which are the plant's primary photosynthetic organ.

The stipe grows to a length approximately equal to the water's depth (typically 5–20 m) and the buoyancy of the pneumatocyst ensures that the blades are held near the water's surface where light is most intense. Together the stipe and blades are referred to as a frond. Unlike other giant kelps such as *M. pyrifera* (figure 1), *N. leutkeana* has only one frond per holdfast and one compact pneumatocyst per frond, and it is this simplicity of structure that makes the bull kelp a compelling model with which to begin our exploration of kelp mechanics.

On the coasts of California, *N. leutkeana* is found only on the most wave-exposed shores; it is supplanted by *M. pyrifera* at more protected sites. By contrast, in Washington state (where *M. pyrifera* is not found), *N. leutkeana* can be found in both exposed and protected sites (Johnson & Koehl 1994).

Nereocystis leutkeana is an annual plant. Microscopic gametophytes shed their gametes in early spring, and the resulting sporophytes grow at a prodigious rate (up to 25 cm per day), reaching their adult size by early summer. Spores (which form in patches on the blades) are shed in late summer, and the plant senesces and dies during the autumn and winter. This life history allows the plant to avoid the predictably severe hydrodynamic conditions that accompany winter storms, but the plants are nonetheless subjected to the occasional large-wave events that occur in spring and summer.

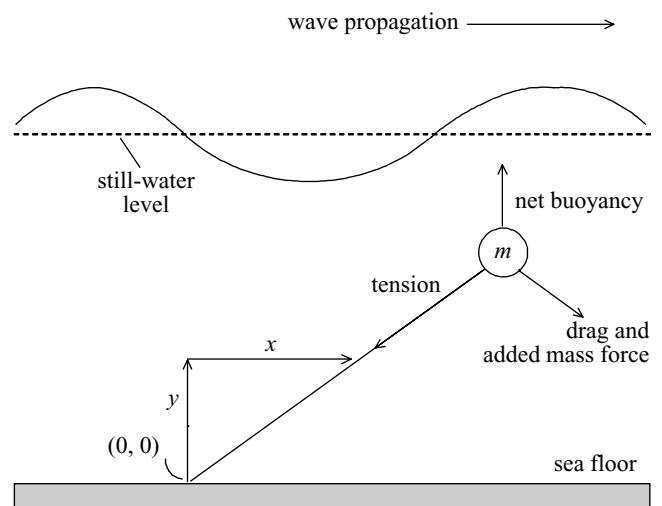


Figure 2. A conceptual drawing of the mathematical model.

In its simplicity, *N. leutkeana* is an admirable model, but it is by no means a practical laboratory organism. To study its mechanics in captivity one would need a tank of seawater 10–20 m deep in which waves at least 2–3 m high could be produced, an apparatus well past the reach of current biological research budgets. Instead, the mechanics of *N. leutkeana* must be studied either in the field or through the use of mathematical models. Both these approaches will be used here.

3. A MATHEMATICAL MODEL

Denny *et al.* (1997) proposed a simple mathematical model of *N. leutkeana* (figure 2). In this model, all of the forces that act on the real frond are assumed to act at a single point. For example, this point element has the same mass, m , as the combined stipe and blades of a real plant, and this mass is accelerated only if a net force is applied. There are five forces that potentially contribute. First, the point element is subjected to the net vertical buoyancy of the frond, F_b , the difference between the weight of the plant in water and the buoyancy of the pneumatocyst. In addition, if the water accelerates relative to the sea floor, a pressure gradient must be present, and the point element is consequently subjected to a virtual buoyancy, F_{vb} . F_{vb} acts in the direction of the water's acceleration. If water moves relative to the point element, hydrodynamic forces are imposed on the element. The relative velocity between the water and the element leads to a drag force, F_d , acting in the direction of relative flow. Although for the purposes of the model drag is assumed to act at the point element, the magnitude of drag is proportional to the blade area of a real bull kelp. Relative acceleration between the element and the surrounding water imposes an accelerational force, F_a , often referred to as the acceleration reaction. Again, while in the model F_a acts at the point element, its magnitude is proportional to the size of the actual plant, in this case to the frond's volume. Lastly, the point element can be subjected to a tensile force by the stipe. To this end, the stipe is assumed to act as an elastic rope of unstretched length, L , that tethers the point element to the origin of a coordinate system ($x=0$, $y=0$) located on the sea floor. If distance from the point element to the

origin, $d = \sqrt{x^2 + y^2}$, is less than L , no force is applied by the stipe. If d is greater than L , a tensile force, F_t , is imposed, directed toward the origin. The magnitude of F_t increases in proportion to $d - L$. In all cases, the relevant characteristics of the plant (unstretched stipe length, blade area, plant volume and net buoyancy) and the constants of proportionality (the shape coefficient of drag, the added mass coefficient and the elastic modulus of the stipe material) are taken from measurements made on actual *N. leutkeana* fronds.

With this list of forces in hand, the equation of motion for the point element can be written

$$a = (F_b + F_{vb} + F_d + F_a + F_t)/m, \quad (3.1)$$

where a is the acceleration of the point element, and both a and all of the forces are assumed to be vector quantities. For the details of this equation, consult Denny *et al.* (1997) or Denny *et al.* (1998).

This simplified model of a giant kelp frond is then placed into a hypothetical ocean in which it can be subjected to the water motions that accompany idealized waves. For the sake of simplicity we have chosen to use linear wave theory to describe the flow field generated by ocean waves. Using this simple theory, we can specify the water velocity and acceleration for any location of the model kelp's point element as a function of time (see Kinsman 1965; Denny 1988). From this information, the magnitude of the various forces acting on the point element can be determined, and the equation of motion can be integrated through time to provide a description of the temporal pattern of velocities and locations for the point element.

Of particular interest in this calculation is the pattern in which the stipe is stretched. For a plant firmly anchored to the substratum by its holdfast, the stipe is the weakest link in the frond. If the tension in the stipe exceeds the strength of the stipe's material, the stipe breaks and the plant is cut loose to die when it is washed up on a beach. Thus, the practical result of this model is a prediction of the tension in the kelp's stipe as a function of the size and shape of the plant, the stiffness of the stipe, the depth of the water, and the height and period of the waves.

The detailed results of this model are described in Denny *et al.* (1997). In brief, they suggest that the tension acting on the stipe is a result of two counteracting aspects of the kelp's kinetics. First, the flexibility of the rope-like stipe allows the frond to move with the flow, thereby decreasing the water's velocity and acceleration relative to the plant. This reduction in relative motion results in a reduction in hydrodynamic force, and thereby a reduction in the tension required to keep the plant tethered (an effect predicted by Koehl 1984, 1986). The ability to 'go with the flow' is not without negative ramifications, however. In moving with the surrounding water, the mass of the frond attains considerable momentum. If during the passage of a wave the plant comes to the end of its tether, this momentum applies a large decelerative 'jerk' to the stipe. It is this inertial force, rather than the forces due directly to drag or the hydrodynamic acceleration reaction, that is predicted to be the largest force imposed on *N. leutkeana* and other giant kelps (Denny *et al.* 1998).

However, it is not these results that we wish to concentrate on here. Rather, we desire to explore how this math-

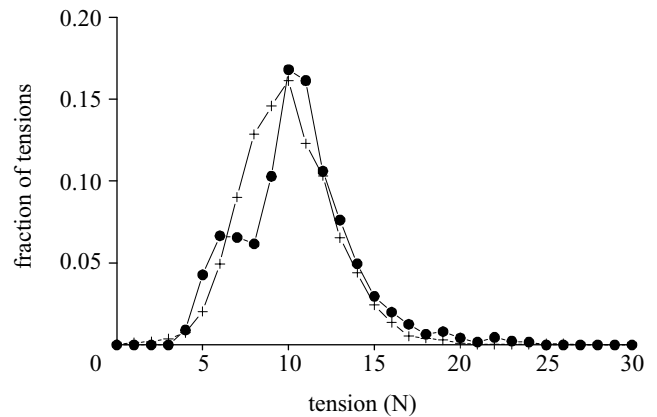


Figure 3. Forces on real and model *Nereocystis leutkeana*: a comparison of the distribution of forces measured in the field (curve with circles) and those predicted by the model (curve with crosses). The average and standard deviations of the two distributions are statistically indistinguishable. To make these predictions, the model was run using the time course of ocean surface elevations recorded in the field and size and shape parameters that were appropriate for the experimental plant. (Reprinted from Denny *et al.* (1997).)

ematical model of plant kinetics can be integrated with other modelling techniques to provide a richer picture of the biology of *N. leutkeana*. We begin with an examination of how the mathematical model can be tested.

4. TESTING THE MODEL

(a) *Limitations of field trials*

The mathematical model of Denny *et al.* (1997) has been tested in two ways. First, measurements of the tension imposed on actual giant kelps in the field, along with simultaneous measurements of wave characteristics, allowed for a comparison of predicted and actual values. On average, the model acquitted itself quite well (figure 3). That is to say, the mean and standard deviations of the forces predicted by the model closely matched those recorded in the field.

This similarity may be misleading, however. A time-series of predicted and measured values shows that while the model can at times closely predict the moment-to-moment pattern of tension in the stipe, there are periods during which the model deviates substantially from reality (figure 4). These deviations are probably due to the overly simple nature of the model. For example, the blades of the actual plant can be several metres long, and therefore will sample the flow field differently than will the point element assumed by the model. Furthermore, in the model the shape coefficient of drag is constant, but in the real plant it may in fact depend on time as blades flutter and sway. Alternatively, the observed deviation between prediction and reality could be due to some basic flaw in the mathematical model or its implementation as a computer program. It is this last possibility that is potentially most disturbing, because it is the most difficult to detect through field experimentation. In the field, each wave is different from the next and the characteristics of waves are not under the experimenter's control. As a consequence, each wave amounts to a separate, unrepeatable experiment; a less-than-ideal method for comparing predictions

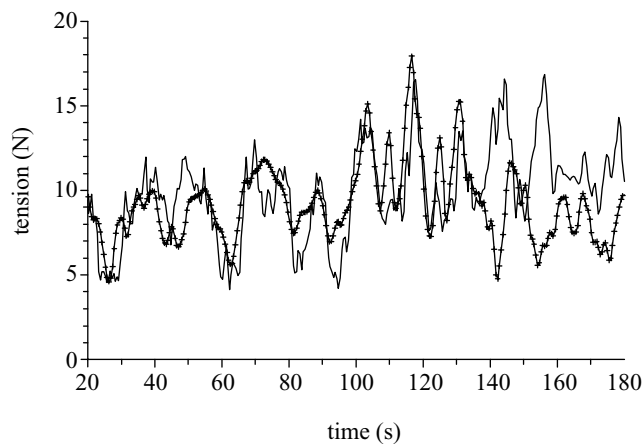


Figure 4. The time-series of forces predicted by the model (curve with crosses) and those measured in the field (solid curve; reprinted from Denny *et al.* 1997). Although the average and distribution of forces are similar between measurement and prediction, at times the model deviates from reality.

with results. It would be preferable to test the model in a controlled situation in which the predictions of the model could be compared with repeated trials. For instance, one surprising prediction of the mathematical model was that a *N. leutkeana* frond would undergo chaotic motion under certain wave conditions if its net buoyancy were artificially decreased (Denny *et al.* 1997). Given the large size of *N. leutkeana* fronds, the kind of controlled experiment required to demonstrate this effect is not feasible on real plants. Instead, we chose to test the mathematical model using a more practical physical model.

(b) *Balls on strings lead to chaos*

Experiments were carried out in a laboratory wave tank in which the period and height of waves could be precisely controlled, and replicate waves could easily be produced (Denny *et al.* 1997). We submerged in this tank two physical models. Each was a table tennis ball attached to an elastic string, an obvious analogy to the ball-on-a-string form of the mathematical model (figure 2). In one case, the ball was filled with air, resulting in a high buoyancy and a simple pendulum-like behaviour when the model was subjected to waves. In the second case, the ball was filled with corn oil, which reduced its buoyancy and led to a much more complicated motion. In both cases, the appropriate 'morphological' measurements (diameter and volume of the ball, net buoyancy, length and stiffness of the string) and hydrodynamic parameters (drag and added mass coefficients) could be measured directly from the physical models or taken from the engineering literature.

Each physical model was subjected to a monochromatic wave train with measured height and period, and the motion of the ball was recorded using a video camera. These recordings could then be analysed to provide a time-series of the location of the centre of mass of the ball every 0.033 s. This record (which amounted to hundreds of repeated trials of the same experiment) could be compared with the predictions of the mathematical model, made using the parameters for the ball and string. A variety of comparisons are possible. At any time, the location, velocity and acceleration of the physical ball can be com-

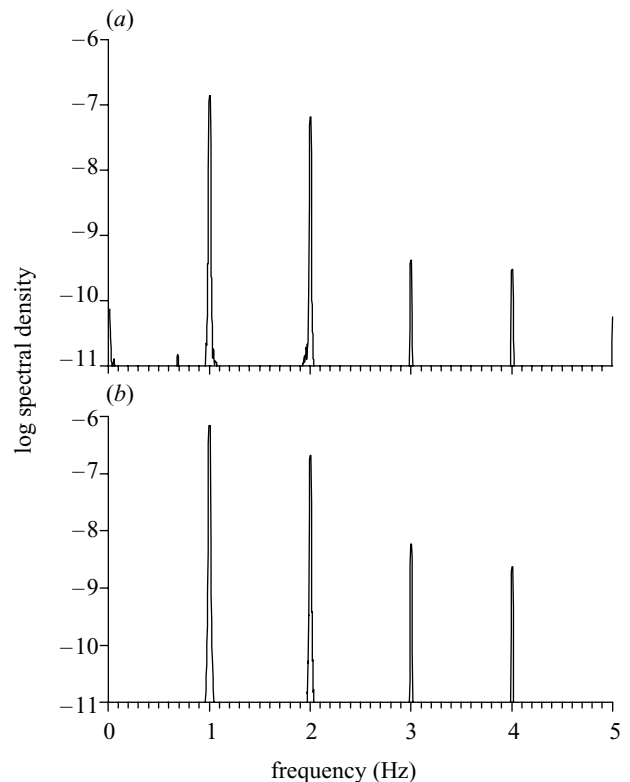


Figure 5. Spectra of lateral motion for the air-filled ball on a string. The predictions (b) and measurements (a) match well. Both the physical and mathematical models were subjected to waves with a period of 1.0 s. (Reprinted from Denny *et al.* (1997).)

pared with the comparable data for the point element in the mathematical model. Alternatively, the time course of the experiment can be included in the comparison through the use of spectral analysis.

The results were encouraging. The simple motion of the buoyant ball was closely predicted by the mathematical model. For example, the spectra of the measured and predicted motions are virtually identical (figure 5). The oil-filled (and therefore less buoyant) ball exhibited the surprisingly complex motion anticipated by the mathematical model. Occasionally, the jerk when the ball reached the end of its tether, coupled with downward flow from the waves, would drive the ball down toward the floor of the tank. The ball would then slowly float upward while its string was slack. Eventually the ball would again come taut on its string, but its subsequent motion was extremely sensitive to the timing of this jerk relative to the phase of the wave. This unpredictable, chaotic motion of the physical model is mimicked by the mathematical model. For example, the spectrum of the motion of the physical ball (figure 6a) reveals considerably broadband variance at frequencies well below that of the waves (1.5 Hz), as does the corresponding spectrum based on the mathematical model (figure 6b). The details of these comparisons are explained by Denny *et al.* (1997), as is the evidence that the motion of both the oil-filled ball and its mathematical model are indeed chaotic. These results from a laboratory-based physical model provide the best evidence to date that the basics of our mathematical model of *N. leutkeana* are not seriously flawed, and suggest that the deviation between the predictions of the model and the forces meas-

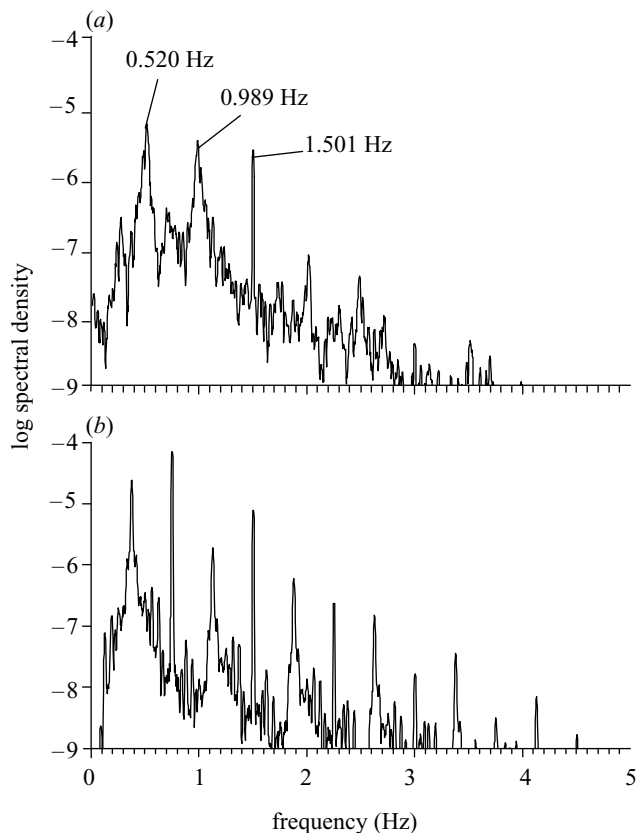


Figure 6. Spectra of lateral motion for the oil-filled ball on a string. Both the measured spectrum (a) and the predicted spectrum (b) show broadband variance at frequencies well below the wave frequency (1.5 Hz)—a characteristic of chaotic motion. (Reprinted from Denny *et al.* (1997).)

ured on kelps in the field (figure 4) are due to the overly simple nature of the current model.

With this thought in mind, an obvious next step would be to tinker with the mathematical model, adding in more detail. For example, by treating the model kelp as a series of linked point elements, it would be possible to incorporate into the model the distributed load placed on actual plants and allow for relative motion between the pneumatocyst and blades. This approach has been used to model the intertidal kelp, *Egrecia menziesii* (Friedland & Denny 1995). More realistic flow fields could be incorporated into the model, potentially including the effects of wave breaking. However, this tinkering would amount to a fine tuning of the model, not a new use of the model *per se*. For our purposes here we turn our attention to the ways in which the current model (limited as it may be) can be used in novel ways, for example, to explore the mechanical properties of kelp stipes.

5. EXPLORING MATERIAL PROPERTIES

The rough evaluation described in § 4 suggests that when our mathematical model has been provided with the size, shape and material properties of the plant, it does an adequate job of predicting the forces imposed on a kelp. If we choose to trust the model, we can then use it to explore how variations in these characteristics could affect the imposed force. Variations in size and shape have been treated by Denny *et al.* (1997) and will not be discussed

here. Instead, we use the model to provide insight into how any variation in the material properties of the stipe would affect the extension and force to which the stipe is subjected, and thereby how the material properties affect the probability that the stipe will be broken.

Four parameters are used to describe the mechanical state of stipe material (see Wainwright *et al.* (1976) or Denny (1988) for a more thorough explanation of these parameters). The tensile force applied to the stipe is normalized to the stipe's cross-sectional area to give the *stress* (measured in pascals). The extension of the stipe ($d - L$) is normalized to the unstretched length of the stipe (L) to give the *strain*. The ratio of stress to strain is a measure of the material's *stiffness* or *elastic modulus*. And finally, the integral of the product of stress and strain gives a measure of the energy per volume required to extend the material. This is the *strain energy density*.

The mechanical properties of *N. leutkeana* stipe material have been examined by Koehl & Wainwright (1977), Johnson & Koehl (1994) and Hale (2001). In brief, the material can be extended by *ca.* 30% of its unstretched length (a strain of 0.30) before it breaks, and it has a breaking stress of 3–5 MPa. The stiffness of the material varies with strain, but at the small strains that typically result from wave-imposed forces, the elastic modulus is 10–40 MPa. The average stiffness for stipes collected from 10 m depth around the Monterey Peninsula is *ca.* 40 MPa, and this is the stiffness value used in the mathematical model.

However, the stiffness of algal materials varies dramatically among species, from a low of *ca.* 0.2 MPa for the red alga *Nemalion* to a high of *ca.* 200 MPa for *Pterygophora* (Hale 2001). How different would the imposed force and extension be for a bull kelp if its stipe material had a different stiffness? This question can easily be addressed with our mathematical model, and representative results are shown in figure 7. Here, we have plotted the safety factor for the stress, strain and strain energy density, each as a function of the stiffness of the stipe. For our purposes, the safety factor is defined as the ratio of the imposed value of stress, strain or strain energy density to the breaking value measured in the extant material of *N. leutkeana*. For example, a typical breaking stress for *N. leutkeana* stipes is 3 MPa. If for a given stipe stiffness and wave height the model predicts that a stress of 1 MPa will be imposed, the safety factor for this stiffness and wave height is 3. The range of elastic moduli shown on the abscissa of this graph encompasses the range of stiffnesses measured in marine algae (Hale 2001).

Under the flow conditions used in this typical case (a wave height of 5 m and a wave period of 10 s), the higher the modulus of the material, the larger the tensile stress imposed on the stipe, and the lower its safety factor. This effect is due in large part to the fact that it is the inertial force acting when the frond mass comes to the end of its tether that imposes the bulk of the force. In this respect, the stipe of a bull kelp is predicted to behave much like a mountain climber's rope. If the climber falls, his mass attains a substantial kinetic energy that is eventually absorbed by the rope when he comes to the end of his tether. The energy absorbed is proportional to the tensile force applied by the rope times the distance through which the force is applied. As a consequence, the stiffer the rope,

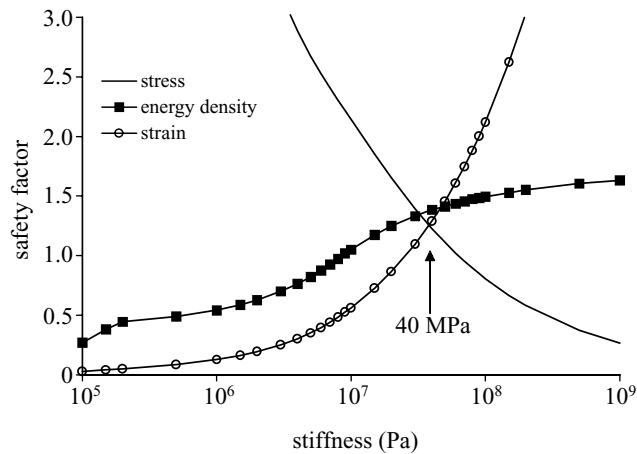


Figure 7. Safety factors for a mature adult kelp at a wave height of 5 m. The safety factors for the strain and strain energy density both decrease with increasing stipe stiffness, whereas the safety factor for stress increases with increasing stipe stiffness. The stiffness at which the lowest of these three safety factors is maximized lies very close to the measured stiffness of *Nereocystis leutkeana* stipes, suggesting that the mechanical properties of the stipe have been tuned to the hydrodynamic environment. (Data from Hale (2001).)

the shorter the distance over which the climber is jerked to a halt, the larger the force to which the rope is subjected, and the lower the rope's factor of safety. It is for this reason that climbing ropes are relatively stretchy; a stiffer rope would be more likely to break both the rope and the climber. The kinetics of *N. leutkeana* are actually a bit more complicated. Unlike a falling climber at the end of his rope (for whom the kinetic energy is maximal), a kelp frond continues to interact with the surrounding fluid throughout its deceleration. Kinetic energy can be transferred to or from the water through the action of drag and the acceleration reaction, and this interaction can in theory either augment or reduce the force imposed on the stipe (see Gaylord *et al.* 2001). Nonetheless, for the conditions used in our model, the analogy to a climbing rope is appropriate.

If high stiffness leads to low safety factors, why are the stipes of giant kelps so stiff? There are many algae with more compliant stipe materials. Would use of these materials in the bull kelp reduce the risk of breakage? Not necessarily, because tensile stress is not the only consequence of an applied force that can lead to breakage of the stipe. As figure 7 implies, there are at least two additional factors that must be taken into account. First, if the stipe's material is stretched beyond its strain limits (regardless of the applied force), the material will break. Second, the elastic potential energy stored by the stipe as it is extended can fuel the propagation of fatigue cracks in the material, eventually leading to failure. Thus, it could be advantageous for the stipe to minimize strain and strain energy density, thereby maximizing their safety factors. Figure 7 shows, however, that the safety factors for both strain and strain energy density behave in a manner opposite to that of applied stress: they are low when the stiffness of the stipe material is low and are high when the stiffness is high. The competing trends between stress on the one hand (the lower the stiffness the higher the stress safety factor) and strain and strain energy density on the

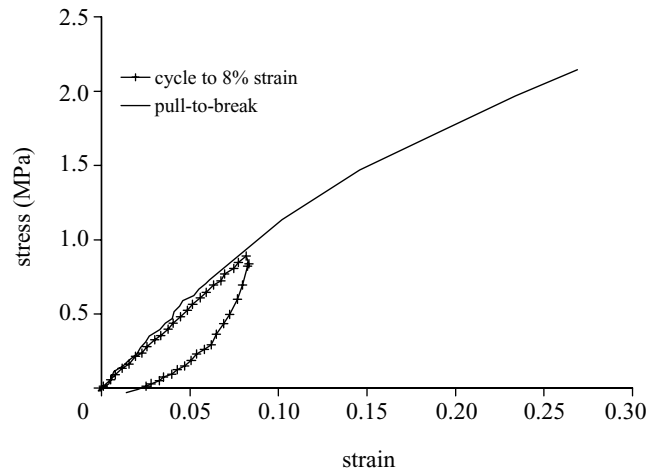


Figure 8. Representative cyclic stress–strain curves for *Nereocystis leutkeana*. The stiffness of the material depends on how far it has been deformed, and considerable hysteresis is evident.

other (the lower the stiffness the lower the safety factor) lead us to suppose that the overall 'best' stiffness for the stipe material is found at an intermediate level. Indeed, the stiffness at which the combined safety factors for stress, strain and strain energy are maximized (38.4 MPa) is tantalizingly close to the measured stiffness of *N. leutkeana* stipe material (37.1 MPa).

As tempting as it would be to accept these results at face value, we are sceptical. First, the safety factors depicted in figure 7 have been calculated using fixed values for breaking stress, strain and strain energy density, values measured for the existing stipe material. In fact, if the kelp evolved a material with a different stiffness, its breaking stress, breaking strain and breaking strain energy density could not all stay the same. For example, if the average stiffness of the material increases, but it has the same breaking strain, it must have a higher breaking stress. Thus, unless we can find a method to predict how stiffness, breaking stress, breaking strain and breaking strain energy density would covary through the course of evolution, the precise form of figure 7 must remain suspect. In this regard, the calculations shown in figure 7 push the mathematical model to (and perhaps beyond) its current practical limits.

The results shown in figure 7 are suspect for another reason as well. In making these calculations we have assumed that the stipe material acts as an elastic solid. That is, we have assumed that the tensile force imposed by the stipe on the point element is linearly proportional to the extension of the stipe beyond its unstretched length, and that all the energy expended in extending the stipe can be recovered as the stipe returns to its resting length. However, Johnson & Koehl (1994) and Hale (2001) have shown that the behaviour of *N. leutkeana* stipe material is not so simple (figure 8). First, as we have noted above, the stiffness of the material is itself a function of strain; the stipe is stiffest at low strain, and its modulus decreases as the stipe is extended. Furthermore, the material is not entirely elastic; some of the energy required to extend the stipe is dissipated internally during extension (in a process known as hysteresis), and as a result, the path of the stress–strain curve is different when the stipe is being

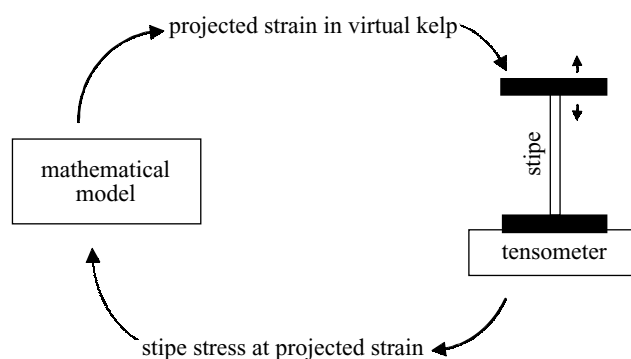


Figure 9. A conceptual drawing of the cyberkelp apparatus.

returned to its resting length from when it is being stretched. In many cases the material is plastically deformed during extension (its resting length after being extended is longer than before), and the precise manner in which stress varies with strain is sensitive to both the history of strain and the rate of strain. In other words, the properties of *N. leutkeana* stipe material are complex, and it seems likely that these complexities could have a substantial effect on the kinetics of the kelp in flow. How can the complex mechanical behaviour of the stipe be incorporated into our mathematical model?

The traditional approach to this question is not encouraging. It consists of a laborious compilation of the material properties under a wide range of strains, strain rates and strain histories in the hope that within this compendium of data sufficient information will be present to inform the model of the appropriate parameters as they are encountered. However, without prior knowledge of what strains, strain rates and strain histories the model will encounter, one is likely to make many more measurements than is necessary. Prior knowledge of the plant's kinetics would reduce the measurements we would need to characterize the material properties. But this line of reasoning leads to a biomechanical 'catch-22'. We need to know the plant's kinetics to be able to measure the material properties efficiently, but we need to know the material properties to predict the kinetics.

6. CYBERKELP

We have managed to sidestep this conundrum by combining our mathematical model with a computer-controlled materials testing apparatus (Hale 2001). An outline of the resulting 'cyberkelp' is shown in figure 9. The mathematical model numerically integrates the equation of motion through time as described in § 5. However, when the model reaches the point in the calculation at which it previously would have applied a strain to the numerical stipe, it now suspends the calculation briefly (for *ca.* 50 ms), and instructs the testing apparatus to strain an actual sample of *N. leutkeana* stipe. The resulting force is measured, digitized and fed back to the computer, which then resumes its numerical integration. In this fashion, the time course of strain on the kelp material is similar to that which would occur under field conditions, but because the material is held in the testing apparatus, we can record the time-series of stress and strain, from which the appropriate

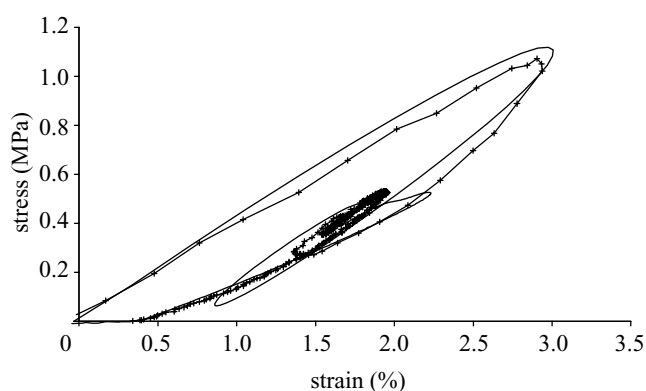


Figure 10. Stress–strain curves for a *Nereocystis leutkeana* stipe tested in the cyberkelp system (curve with crosses) and standard linear model (curve without crosses), both under simulated 7 m waves. The strain for the *N. leutkeana* stipe has been shifted 0.94% to the left (the amount of permanent plastic strain in the stipe) to align the traces.

materials properties (modulus, hysteresis, plastic strain, etc.) can be calculated.

Representative results are shown in figure 10. The predominant stress–strain loop is that due to the plant jerking on the end of its tether. The secondary loops are a result of the frond mass oscillating in a damped resonance after the initial jerk. Of particular interest is the ability of the material to dissipate energy during this loading regime. Using cyclic tests at a constant strain rate, Johnson & Koehl (1994) demonstrated that *N. leutkeana* stipe material is very nearly elastic at the low strains imposed by waves. That is, when tested at a constant strain rate, the stress–strain curve during repeated extensions is nearly the same as the stress–strain curve during recovery. In our tests of *N. leutkeana* stipes on the Monterey peninsula, the area within the stress–strain loop (a measure of the strain energy dissipated) is small, only *ca.* 16% of the total area under the extension curve. By contrast, when the material was loaded as it would be in nature, the fraction of energy dissipated (the hysteresis) is substantially higher (*ca.* 41%).

This high hysteresis under simulated wave conditions may be functionally important to the kelp. Under all but the largest waves possible, the stress applied to the stipe is predicted to be well below the breaking stress. Thus, under typical wave conditions, the plant would not be expected to break as a result of the passage of a single wave. But ocean waves are continuous. Given a typical wave period of 10 s, a plant is subjected to 8640 waves per day. If the stipe material were capable of efficiently storing elastic potential energy, this energy could cause the material to fatigue through the propagation of cracks (Denny *et al.* 1989; Hale 2001). We speculate that the likelihood of fatigue failure is reduced by the high hysteresis described already. Note that it is doubtful whether this property of *N. leutkeana* stipe material would have been recognized through the use of more traditional testing methods.

7. A RETURN TO MATHEMATICAL MODELLING

Having empirically measured the behaviour of stipe material under simulated wave loading, we are now in a

position to model this behaviour numerically. To this end, we employ the standard linear solid, a mathematical representation of a viscoelastic material that consists of a Maxwell element (a spring in series with a dashpot) coupled in parallel with a spring. As shown in figure 10, given appropriate values for the spring stiffnesses and the viscosity of the dashpot (values gleaned from the cyberkelp tests), this simple mathematical solid behaves much as the real material would (Hale 2001). This numerical material can then be incorporated into the overall mathematical model of *N. leutkeana* to improve its predictive capabilities without the need to have the model physically tied to a real piece of material.

At this point our modelling exercise has come full circle. A simple mathematical model has been used as the basis for realistic, empirical tests of the material properties of *N. leutkeana* stipe. These results in turn allow for an improved version of the mathematical model, and potentially for a new round of exploration into the kinetics of giant kelps.

The modelling efforts reported here were supported by NSF grants nos. OCE 9633329 and OCE 9985946 to M.W.D., and by the Partnership for Interdisciplinary Study of the Coastal Ocean (PISCO). This is contribution no. 92 of PISCO.

REFERENCES

- Abbott, I. A. & Hollenberg, G. J. 1976 *Marine algae of California*. Stanford, CA: Stanford University Press.
- Bell, E. C. & Gosline, J. M. 1996 Mechanical design of mussel byssus: material yield enhances attachment strength. *J. Exp. Biol.* **199**, 1005–1017.
- Currey, J. D. 1978 The effects of drying on the strength of mussel shells. *J. Zool. Lond.* **188**, 301–308.
- Denny, M. W. 1988 *Biology and the mechanics of the wave-swept environment*. Princeton University Press.
- Denny, M. W. 1995 Predicting physical disturbance: mechanistic approaches to the study of survivorship on wave-swept shores. *Ecol. Monogr.* **65**, 371–418.
- Denny, M., Brown, V., Carrington, E., Kraemer, G. & Miller, A. 1989 Fracture mechanics and the survival of wave-swept macroalgae. *J. Exp. Mar. Biol. Ecol.* **127**, 211–228.
- Denny, M. W., Gaylord, B. P. & Cowen, E. A. 1997 Flow and flexibility. II. The roles of size and shape in determining wave forces on the bull kelp *Nereocystis leutkeana*. *J. Exp. Biol.* **200**, 3165–3183.
- Denny, M. W., Gaylord, B., Helmuth, B. & Daniel, T. L. 1998 The menace of momentum: dynamic forces on flexible organisms. *Limnol. Oceanogr.* **43**, 955–968.
- Foster, M. S. & Schiel, D. R. 1985 The ecology of giant kelp forests in California: a community profile. *Biol. Rep.* **85** Fish and Wildlife Service of the U.S. Department of the Interior.
- Friedland, M. T. & Denny, M. W. 1995 Surviving hydrodynamic forces in a wave-swept environment: consequences of morphology in the feather boa kelp *Egregia menziesii* (Turner). *J. Exp. Mar. Biol. Ecol.* **190**, 109–133.
- Gaylord, B. & Denny, M. W. 1997 Flow and flexibility. I. Effects of size, shape and stiffness in determining wave forces on the stipitate kelps *Eisenia arborea* and *Pterygophora californica*. *J. Exp. Biol.* **200**, 3141–3164.
- Gaylord, B., Hale, B. B. & Denny, M. W. 2001 Consequences of transient fluid forces for compliant benthic organisms. *J. Exp. Biol.* **204**, 1347–1360.
- Goldenberg, S. B., Landsea, C. W., Mestas-Nuñez, A. M. & Gray, W. M. 2001 The recent increase in Atlantic hurricane activity: causes and implications. *Science* **293**, 474–479.
- Hale, B. B. 2001 Materials properties of marine algae and their role in the survival of plants in flow. PhD thesis, Stanford University.
- Johnson, A. S. & Koehl, M. A. R. 1994 Maintenance of dynamic strain similarity and environmental stress factor in different flow habitats: thallus allometry and material properties of a giant kelp. *J. Exp. Biol.* **195**, 381–410.
- Kawamata, S. 1998 Effect of wave-induced oscillatory flow on grazing by a subtidal sea urchin, *Strongylocentrotus nudus* (A. Agassiz). *J. Exp. Mar. Biol. Ecol.* **224**, 31–48.
- Kawamata, S. 2001 Adaptive mechanical tolerance and dislodgement velocity of the kelp *Laminaria japonica* in wave-induced water motion. *Mar. Ecol. Prog. Ser.* **211**, 89–104.
- Kinsman, B. 1965 *Wind waves*. Englewood Cliffs, NJ: Prentice-Hall.
- Koehl, M. A. R. 1984 How do benthic organisms withstand moving water? *Am. Zool.* **24**, 57–70.
- Koehl, M. A. R. 1986 Seaweeds in moving water: form and mechanical function. In *On the economy of plant form and function* (ed. T. J. Givnish), pp. 603–634. Cambridge University Press.
- Koehl, M. A. R. & Wainwright, S. A. 1977 Mechanical adaptations of a giant kelp. *Limnol. Oceanogr.* **22**, 1067–1071.
- Massel, S. R. & Done, T. J. 1992 Effects of cyclone waves on massive coral assemblages on the Great Barrier Reef: meteorology, hydrodynamics and demography. *Coral Reefs* **12**, 153–166.
- Wainwright, S. A., Biggs, W. D., Currey, J. D. & Gosline, J. M. 1976 *Mechanical design in organisms*. London, UK: Edward Arnold.
- Witman, J. D. 1987 Subtidal coexistence: storms, grazing, mutualism, and the zonation of kelps and mussels. *Ecol. Monogr.* **57**, 167–187.